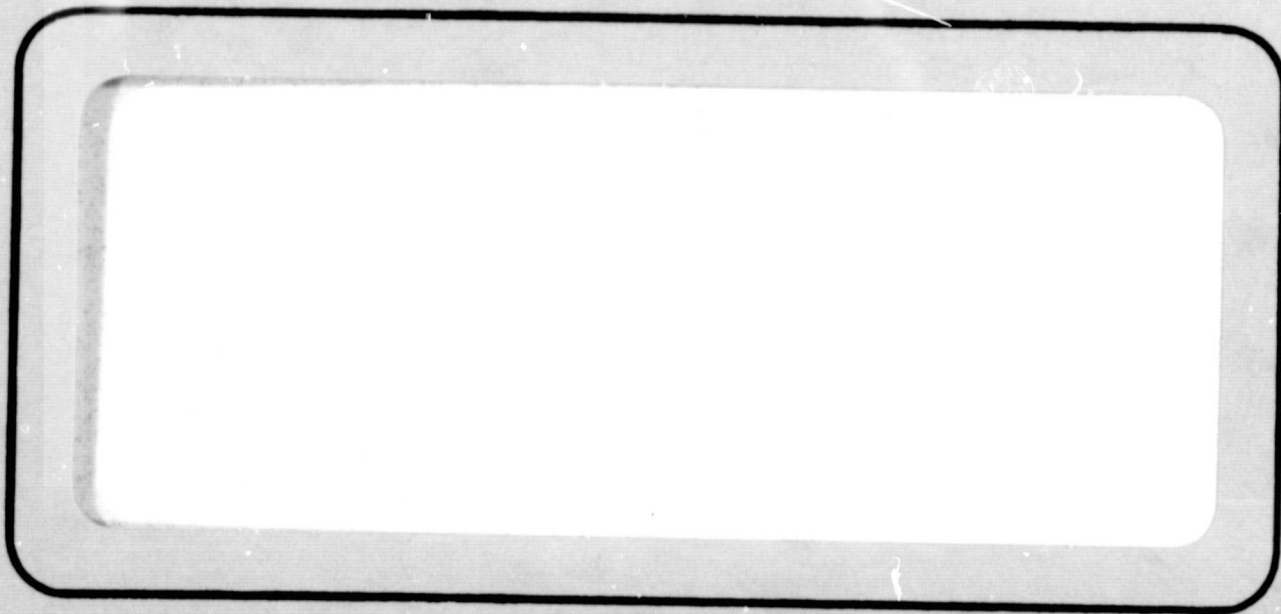


## **General Disclaimer**

### **One or more of the Following Statements may affect this Document**

- This document has been reproduced from the best copy furnished by the organizational source. It is being released in the interest of making available as much information as possible.
- This document may contain data, which exceeds the sheet parameters. It was furnished in this condition by the organizational source and is the best copy available.
- This document may contain tone-on-tone or color graphs, charts and/or pictures, which have been reproduced in black and white.
- This document is paginated as submitted by the original source.
- Portions of this document are not fully legible due to the historical nature of some of the material. However, it is the best reproduction available from the original submission.



**TRW**  
SYSTEMS GROUP

ONE SPACE PARK • REDONDO BEACH, CALIFORNIA



**N69-35473**

FACILITY FORM 602

(ACCESSION NUMBER)

47

(PAGES)

CR-105276

(NASA CR OR TMX OR AD NUMBER)

(THRU)

1

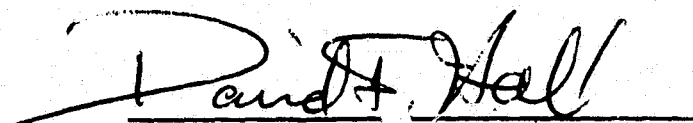
(CODE)

28

(CATEGORY)

Second Quarterly Technical Report  
PROPULSION BEAM DIVERGENCE EFFECTS

Contract No. 952350

A handwritten signature in dark ink, appearing to read "David F. Hall", is written over a horizontal line.

David F. Hall  
Program Manager

This work was performed for the Jet Propulsion  
Laboratory, California Institute of Technology,  
under Contract No. 952350.

TRW Systems  
One Space Park  
Redondo Beach, California  
15 August 1969

#### ABSTRACT

The second phase of a program to develop understanding of and tolerance-level criteria for the deleterious effects of electrostatic rocket exhaust ( $\text{Cs}$ ,  $\text{Cs}^+$ ,  $\text{Hg}$ ,  $\text{Hg}^+$ ) impinging on typical classes of spacecraft surfaces is underway. Prior work was done under Contract No. NAS7-575. This phase includes fabrication of necessary experimental fixtures and exploratory experiments. The current status of fixture design, fabrication, and testing is reported along with early experimental results. Immersion at approximately  $20^\circ\text{C}$  of Teflon FEP, and Kapton (H-film) in liquid  $\text{Cs}$  (but not  $\text{Hg}$ ) and of  $\text{Pb/Sn}$  solder in both  $\text{Cs}$  and  $\text{Hg}$  produced important degradation of sample properties. Sylgard 182, Delrin, GT 100 and SMRD 745, which are representative of additional organic matrices found in spacecraft materials, appeared unaffected by immersion in  $\text{Hg}$  and  $\text{Cs}$ . Silver reacted with  $\text{Hg}$  rather slowly.



This report contains information prepared by TRW Systems under JPL subcontract. Its content is not necessarily endorsed by the Jet Propulsion Laboratory, California Institute of Technology, or the National Aeronautics and Space Administration.

## TECHNICAL CONTRIBUTORS

Electric Propulsion Technology

D. F. Hall

Thermophysics

L. Kelley

Metallurgy

R. Mendelson

Chemistry

R. Meyers

## I. INTRODUCTION

### A. Program Goals

Electrostatic rockets emit propellant particles into at least  $2\pi$  steradians. Spacecraft (S/C) designers therefore require tolerance-level criteria for the almost inevitable interception of propellant particles by S/C surfaces. Under contract NAS7-575 a systematic analytical study was made of the deleterious effects of Hg, Hg<sup>+</sup>, Cs, and Cs<sup>+</sup> on spacecraft surfaces<sup>(1-5)</sup>. Erosion of non-metallic surfaces by sputtering, degradation of thermal control coatings, chemical degradation of non-metallic surfaces, and condensation on solar cell cover glasses are expected to pose the most restrictive design constraints. Of the above areas, quantitative constraints have been generated for condensation; the others are at the qualitative stage and require experimental study.

The program goals of the present effort are 1) to fabricate experimental fixtures required to make these measurements, and 2) perform exploratory experiments to determine in which areas future emphasis should lie.

### B. Program Organization

The program contains four work units: Metallurgy, Chemistry, Thermophysics, and Electric Propulsion Technology. The metallurgy group is charged with elucidating reactions between the propellants and S/C metals. The chemistry group is responsible for elucidating reactions between the rocket efflux and non-metallic S/C materials. The thermophysics group will determine the surface thermal changes which occur in various thermal control coatings. The electric propulsion group is responsible for sputtering experiments, operation of the primary facility in which most exposures are made, and program management.

The structure of this report reflects this program organization.

### C. Program Status

The metallurgical immersion tests are well underway and the chemistry immersion tests have been completed. First experiments on the effects of the propellants on thermal control coatings have begun. The multipurpose sample holder is in the final stages of fabrication.

Unexpected difficulties with the xenon solar simulator (spectral non-uniformity and temporal instability) have resulted in program costs substantially in excess of those planned, as well as some scheduling delays. Therefore the JPL Technical Manager has revised the tentative schedule of experimental activities to reflect a greater emphasis on the high priority thermophysics experiments with mercury, and directed that all work unit budgets be revised to avoid a cost overrun. This is to be accomplished by reduced emphasis on cesium exposures in the 4 x 8 vacuum facility, which have lower priority. Specifically, cesium exposures will be restricted to atoms during the present contract.

Omission of cesium ion beam exposures from this phase of the program is not expected to have serious practical or scientific consequences. The space application of cesium primary thrusters would appear more distant than mercury thrusters. Cesium beam erosion rates will not vary greatly from those of mercury beams, and they probably can be correctly estimated on the bases of measurements with mercury and the relative sputtering yields of those targets reported in the literature. Finally, from a chemical reaction point of view, the impact of an ion on an organic target may be considered to consist of two stages: A reaction which neutralizes the ion and any reaction between the resulting atom and the target. Since mercury atoms are not expected to react with any of the organic materials under study, the planned mercury ion and cesium neutral experiments will provide an interesting "separation of the variables."

## II. TECHNICAL DISCUSSION

### A. Electric Propulsion Technology

1. Summary. Design and fabrication of the multipurpose sample holder was much advanced. Collector plate shields were designed, fabricated and installed. The final mercury gravimetric run was made and the thruster tested. Various improvements and repairs were made in the test facility. Substantial support of thermophysics experiments was rendered. Analysis was made of discharge neutralizers as a source of contaminant particles.

2. Multipurpose Sample Holder. A major effort during the reporting period was completing the mechanical drawings for the multipurpose sample holder and completing the majority of the machine shop work. The final design is believed to satisfy each of six design constraints outlined in the First Quarterly Letter.

All of the basic parts of the multipurpose sample holder have been machined. They are shown completely disassembled in Figure 1 and partially assembled in Figure 2. Removal of individual sample holder "pipes" in a glove bag (following exposure) will be accomplished by removing the screws in the fittings on each end of the pipe and then sliding the pipes forward in the two slotted guide plates. Interposed between adjacent pipes are shields which prevent exchange of sputtered material between them. The rectangular flat copper plates screwed perpendicularly to these shields prevent ions from impacting the shield. Their sides are beveled so that very few atoms of sputtered copper will hit the samples. The sections of thin walled stainless steel tubing between the disconnect flanges and the end plates will minimize the thermal short between pipes, permitting their operation at widely spaced temperatures.

Since the photographs were taken, additional progress has been made in sample holder assembly. The eight stainless steel tubes have been hydrogen brazed to the disconnect flanges and heliarced to the end plates. Special capture screws have been made for the disconnect flanges. Eight fluid vacuum feed throughs and part of the sample guide track were fabricated.

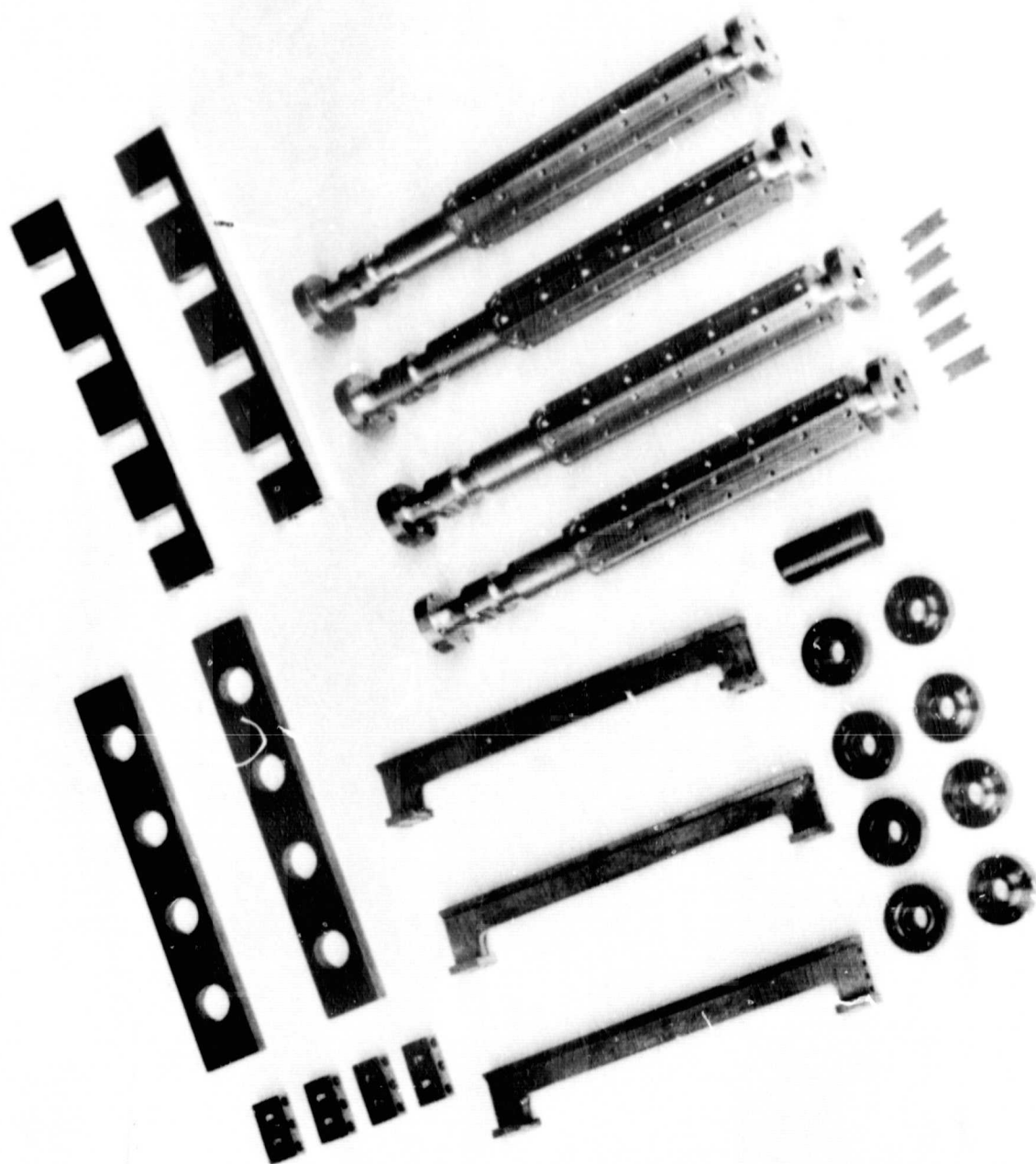


Figure 1. Principal Parts of the Multipurpose Sample Holder.

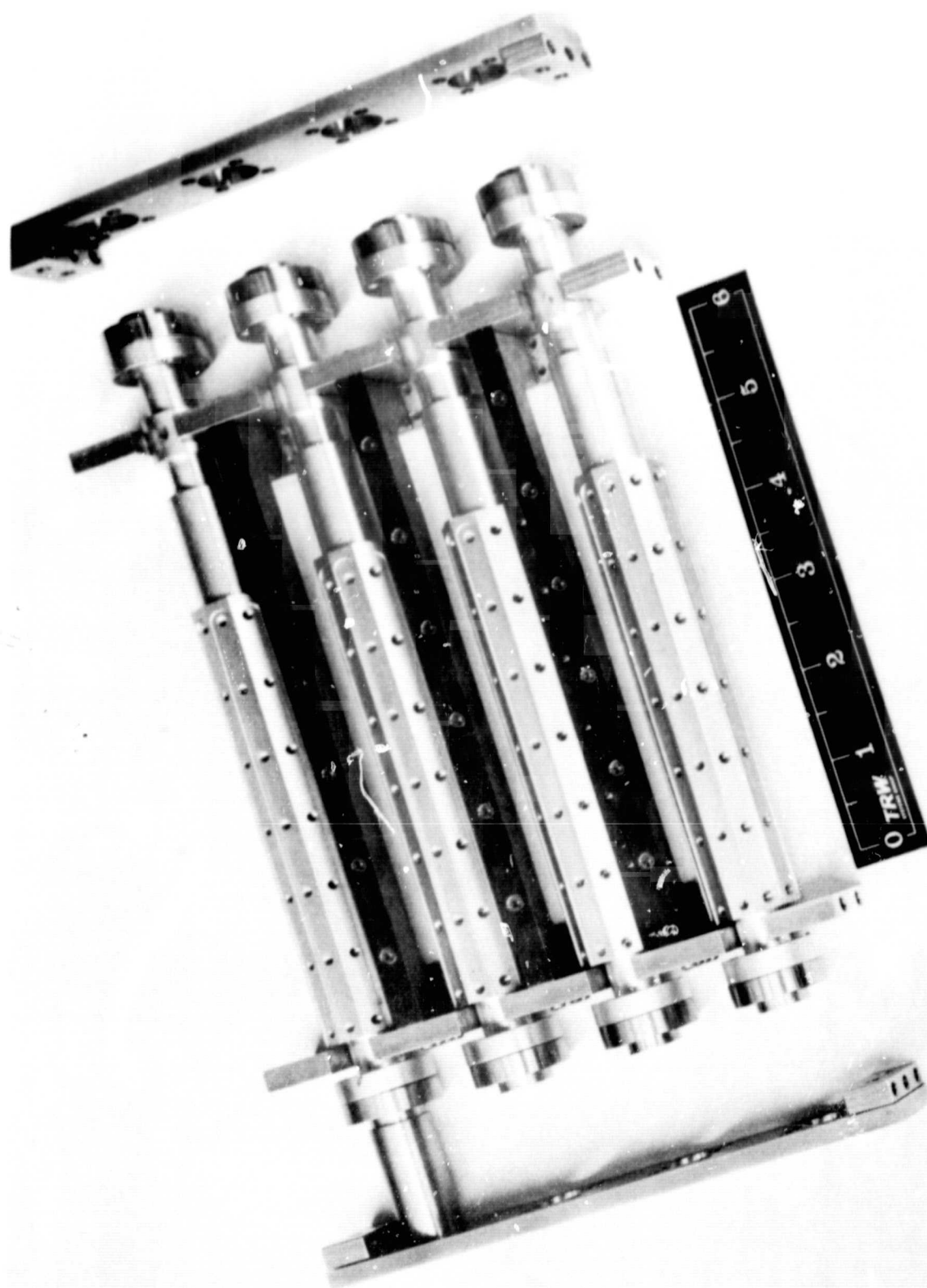


Figure 2. Multipurpose Sample Holder Partly Assembled.



It has been decided that initial use of the sample holder will be with approximately 20°C and approximately 100°C water as the temperature control fluid. These temperatures will be sufficient to allow approximate determination of the activation energy of chemical reactions and establish whether a broader temperature range and/or better temperature control would be a worthwhile investment.

3. Collector Plate Shield. Figures 3 and 4 show the collector plate shields (and the surface thermal sample holder loaded with 5 black paint samples). The forward (most prominent) set shadow the sample area from copper sputtered from the rear half of the cylindrical LN<sub>2</sub> liner shown in Figure 3. The inner set of shields precisely define the sample area and prevent ions from striking the sides of the cut-out in the 5/8 inch thick titanium collector plate. In their absence, sputtered titanium would reach the samples. Both sets of shields have their inside edges beveled to make the edge area, and therefore copper sputtered onto the samples, negligible.

4. Experiments. An additional gravimetric boiler calibration point was obtained for mercury. It is the point at the 6.5 controller set point shown in Figure 5. It now appears safe to ignore the "bad" data point at 6.36.

The thruster was subsequently operated approximately 3 hours to verify that the gravimetric calibration was reasonable, demonstrate the entire system was operating correctly, and to clean the collector following its reinstallation in the tank (see Sect. II.A.6). Acceptable thruster operation was achieved at set points between 7.50 and 7.55 which from Figure 5 corresponds to 300 to 318 equivalent ma and 78.6% to 81% propellant utilization. This utilization is in the correct neighborhood for 15 cm Lewis E-B thrusters of its vintage.

A set of total intensity maps were made of the xenon lamp beam under various conditions. These measurements were motivated by the discovery of spatial nonuniformity in the lamp spectrum reported earlier, and the subsequent observation that the hot lamp electrodes were imaged about a foot in front of the lens. The speculation was that some of the spectral problems related to radiation from these electrodes and that the situation might be improved by masking out the electrode image.

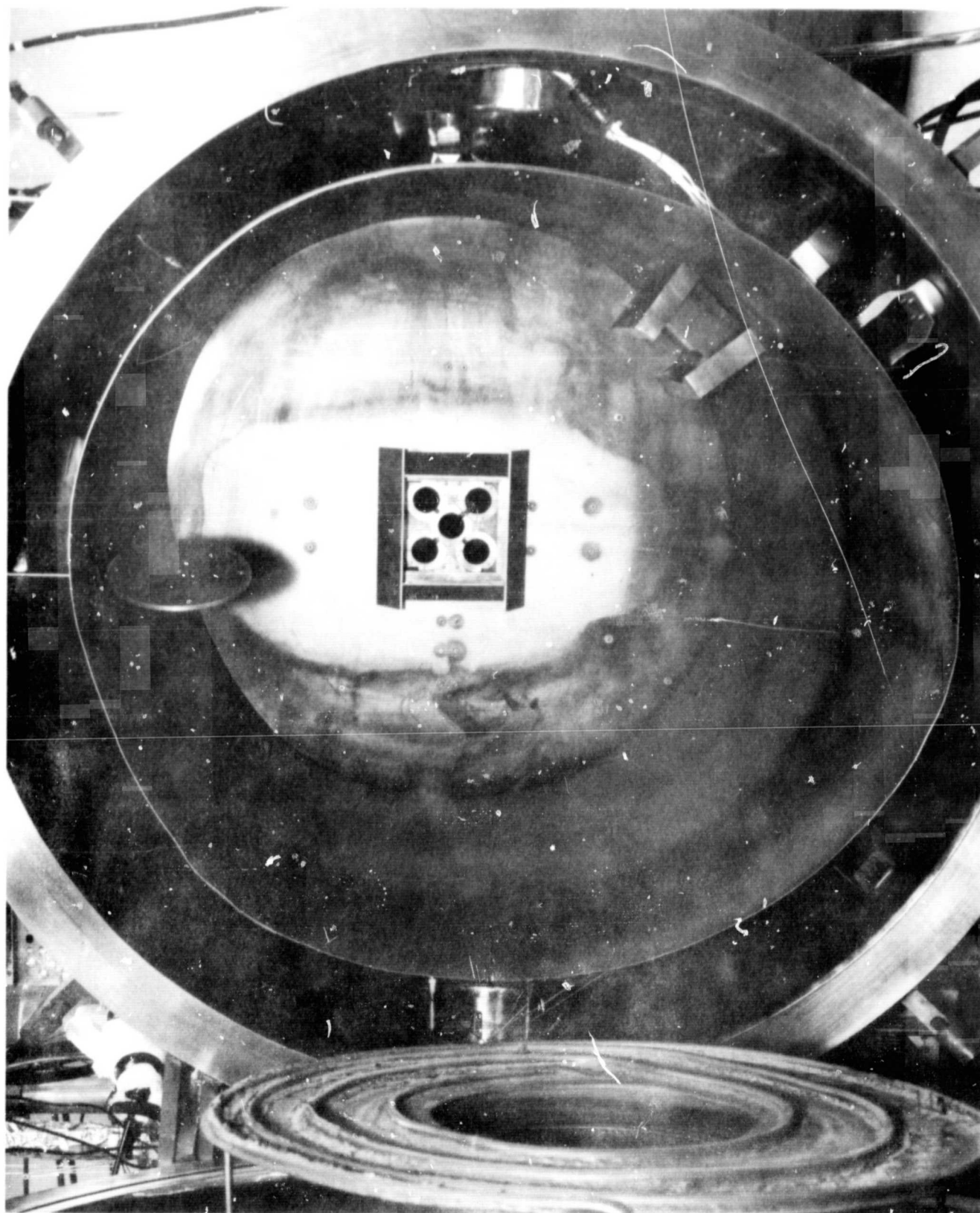


Figure 3. Forward interior Section of 4 x 8 Chamber Showing Front Liner, Titanium Collector, Sputtering Shields, and Surface Thermal Sample Holder in Beam Exposure Position.

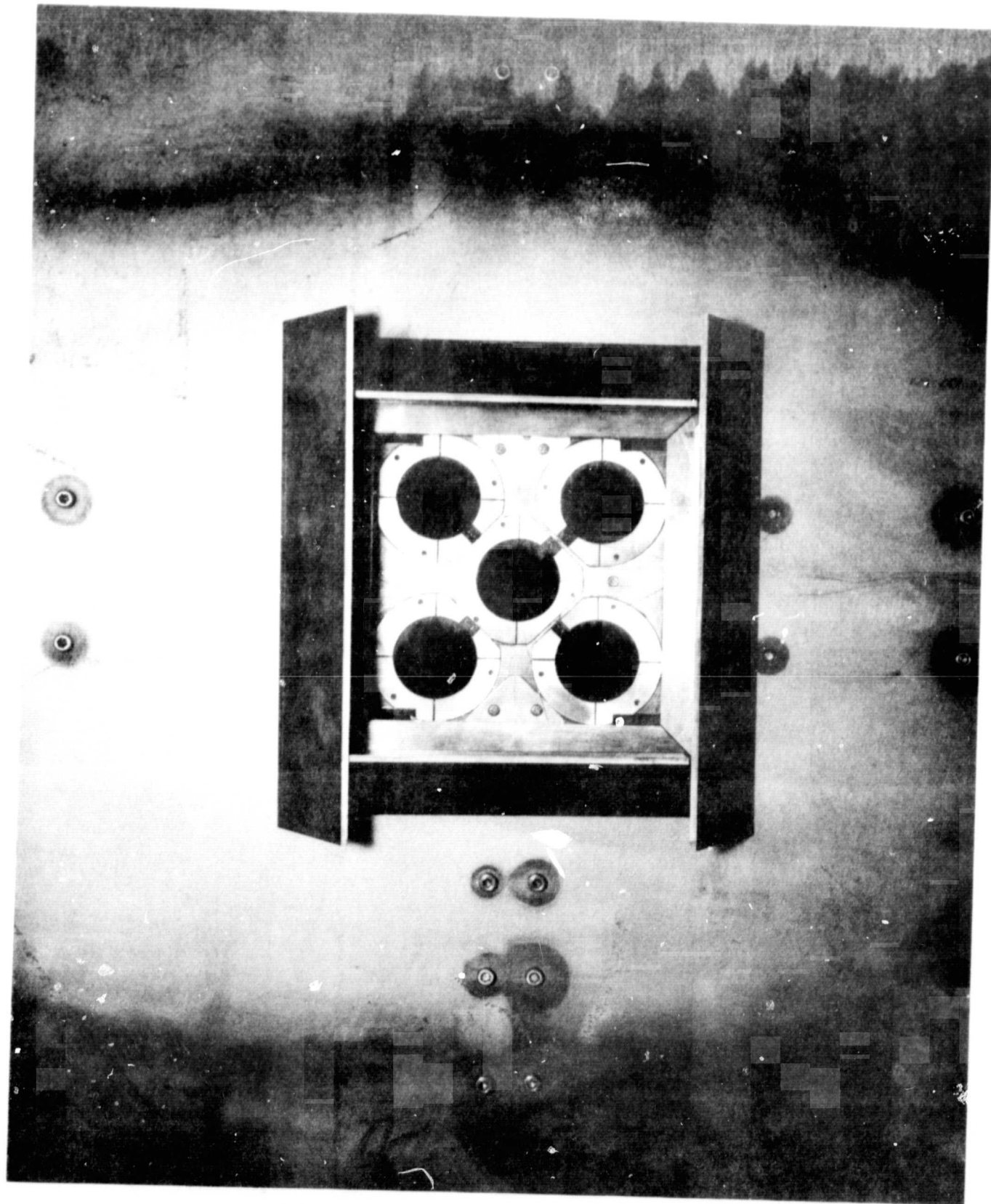


Figure 4. Closeup of Sputtering Shields and Surface Thermal Sample Holder.

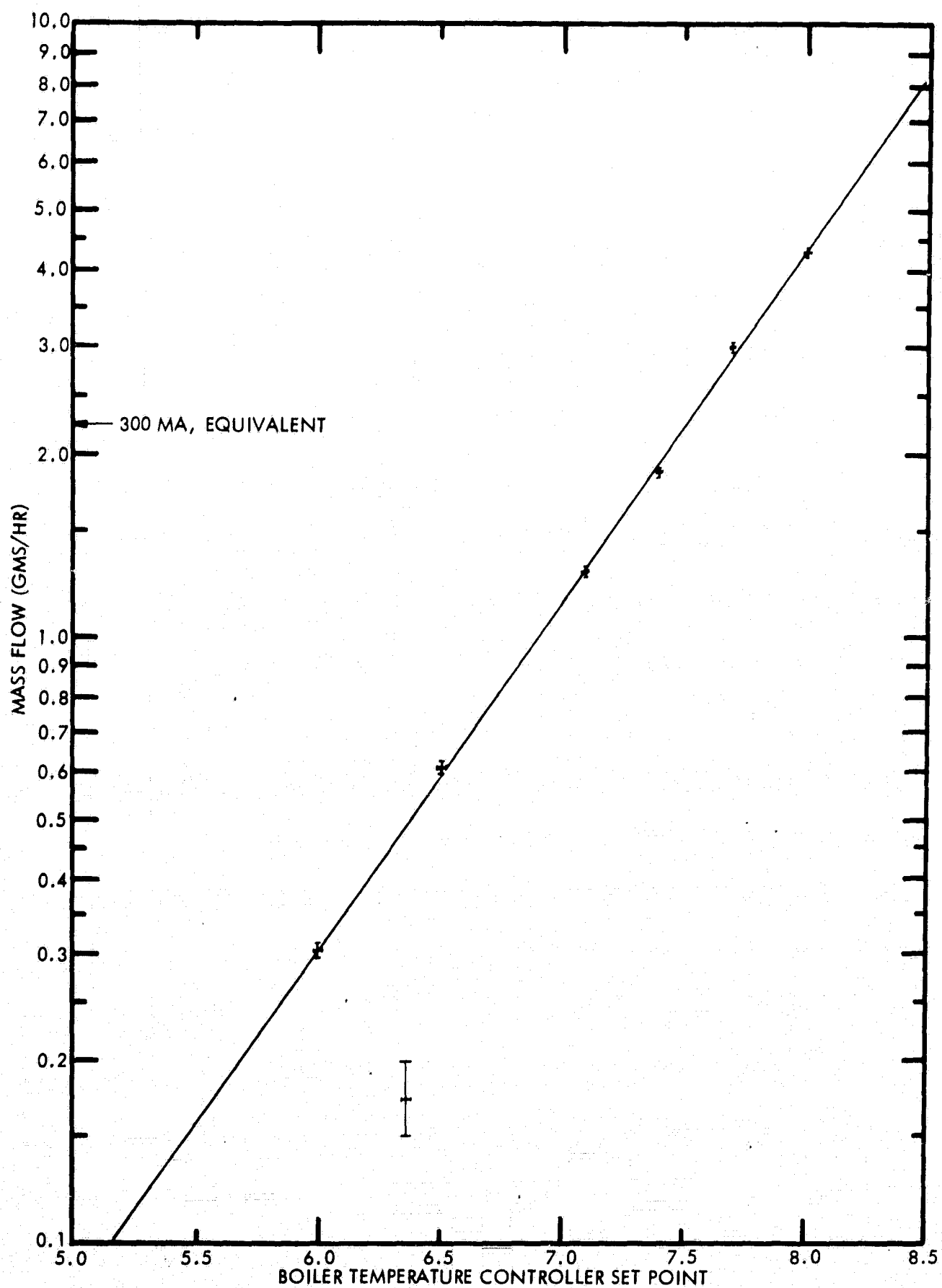


Figure 5. Mercury mass flow from engine boiler vs temperature controller set point.

The measurements showed that with a 9 inch diameter beam on the sample plane the total intensity at corner samples was approximately 60% of that at the center sample. An aperture mask which blocked only the electrode image had minor effect. When the mask was made to intercept the periphery of the discharge image, uniformity of total intensity was increased, but with unacceptable reduction in beam energy arriving at the sample plane.

Therefore attempts to improve the beam quality by masking were abandoned. These results contributed to the decision to use only the central portion of the beam by aiming the lamphouse at individual samples, as described in Section II.B.2

5. Fabrication. A number of fabrication jobs were completed during the period. They are enumerated below:

- (1) Tap water and drain was plumbed to a station near the center port of the vacuum chamber, to provide S-T sample holder cooling. The station has a flow meter, inlet and outlet thermometers, and gate valves. Later this system was modified to permit gravity feed, thereby eliminating pressure fluctuations.
- (2) A section of the rear cylindrical LN<sub>2</sub> shroud was sawed out to permit sample holders to pass behind the collector.
- (3) A fixture which permits anchoring the titanium collector in any selected position was designed, fabricated, and installed. It is necessary to assure that critical sample holder to collector spacings are maintained.
- (4) A control circuit to permit timed bake out of the newly installed foreline trap was designed, fabricated, and installed. Unless this trap is baked after every few chamber evacuations, rough down time is extended.
- (5) The reliability of the thruster electrical vacuum feed-thrus was improved after another user of this design experienced high voltage breakdown.
- (6) The safety and reliability of the test chamber was improved by installing catch-pans under the LN<sub>2</sub> manifold. Previously, the mechanical pumps and floor would get wet from melting ice and frost at the end of each run.

- (7) The EAI 150 quadrupole residual gas analyzer was installed in the chamber. Initial tests indicate that it is performing correctly but is in need of bakeout. We are awaiting delivery of a special heating jacket to perform the bakeout.
- (8) An additional LN<sub>2</sub> solenoid valve and temperature controller were installed on the 4 x 8 facility to feed manifold LN<sub>2</sub> directly to the rear door shroud. Previously this shroud was in series with the rear cylindrical shroud. During testing of the surface thermal sample holder it was found that cool down time was restrictively lengthy. It now takes 1/4 the earlier time.

6. Repair of Titanium Collector. During the reporting period a leak developed in the Ti cooling tube heliarc welded to the rear of the collector. Careful inspection revealed that the plate had begun to crack, starting at one of the sides of the cut-out. When the crack, which was through the 5/8 inch thickness and 1-1/2 inches long, intersected the cooling tube the leak was formed - under the fillet. Therefore the fillet at this location was milled away and the tube patched with a heliarc weld.

This crack in the plate is believed to have resulted from residual stress introduced by the original welding of the tubing to the plate. Therefore a drill hole was made at the apex of the crack to terminate its propagation, and then the plate was sent out for vacuum annealing.

Finally the plate was reinstalled in the chamber and tested. No leaks were found, even after thermal cycling.

7. Support of Thermophysics Experiment. A significant amount of time was expended in solving the temporal instability problem of the solar simulator (see Sect. II.B.9 for additional problem description). Before active regulation was adopted, diagnostic instrumentation was used and the power supply, cables and lamphouse checked for faults. The second power supply tried had relay and mechanical failures, and had to be overhauled before work could proceed.

Electrically, the lamp always displays a positive dynamic resistance at approximately 100 Hz and below. The observed oscillations arise from changes in its characteristic curve with time together with a constant "load line" imposed by the power supply and cables. This oscillatory behavior

is intermittent and was not observed on a similar lamp in operation in the thermophysics laboratory. Therefore the lamp itself is probably defective. However because of the considerable investment made in measuring its spectra, we were loath to replace it or even remove it from the lamphouse. For this reason an electronic shunt regulator using a solar cell sensor was designed, fabricated and demonstrated to provide adequate control of lamp intensity.

In addition to participating in the solution of the lamp problem, the facility was operated for a number of days and aid rendered in the investigation of other experimental problems.

#### 8. Analysis of Discharge Neutralizers as a Source of Contaminant Particles.

Discharge (plasma bridge) neutralizers using both mercury and cesium have been developed, and one or both of these types seem certain to see application in space. These neutralizers emit both atoms and ions (as well as electrons) and therefore constitute a potential source of contaminant particles. The atomic component is considered below, and it is shown that this efflux in a cone about the neutralizer axis may be of significant magnitude.

a. Neutral Efflux. The angular distribution of emitted atoms from the cylindrical neutralizer exit orifice must be of the type described by Clausing.<sup>6</sup> Csiky<sup>7</sup> argues that this distribution probably approaches that of a cosine, considering typical orific dimensions and flow conditions. That assumption is made in the following analysis.

The flux density of atoms arriving at a perpendicular surface a distance  $r$  centimeters from the neutralizer is then given by:

$$\Gamma = 5.3 \times 10^{19} \frac{\dot{m}}{M \cdot r^2} \cos \theta \left( \frac{\text{atoms}}{\text{sec cm}^2} \right) \quad (1)$$

where  $M$  = the atomic weight of the neutralizer propellant in amu  
 $\dot{m}$  = the atomic component of mass flow through the neutralizer in grams/hour  
 and  $\theta$  = the angle formed with the neutralizer axis.



A typical total mass flow rate for discharge neutralizers is 0.3 gm/hr. Part of this flow is emitted as ions, which may give rise to a modified angular distribution. However an estimate of particle current density arriving at a surface may be made by assigning the total neutralizer mass flow to  $\dot{m}$  in Eq. (1). Then on axis ( $\theta = 0$ ) Eq. 1 evaluates

Distance	$\Gamma_{cs}$	$\Gamma_{Hg}$
20 cm	$3 \times 10^{14}$	$2 \times 10^{14}$
5 feet	$5 \times 10^{12}$	$3.3 \times 10^{12}$

The first distance quoted is the diameter of a JPL E-B engine. The second is the minimum distance between thruster and solar panel on the JPL Jupiter Flyby Mission study. Figure 4 and 5 of Reference 5 demonstrates that arrival rates of these magnitudes on the front surface of a solar array may lead to condensation beyond 2.5 AU and 1.6 AU for mercury and cesium, respectively. From another viewpoint, the  $\Gamma_{Hg}$  5' value is equivalent to what one would expect at approximately  $70^\circ$  and 5' distant from the JPL 20 cm E-B thruster.

b. Charge Exchange in the Thrust Beam. In general, the atomic beam described above must pass through the thrust beam before spacecraft surfaces other than the thruster are encountered. If a substantial fraction of the atomic beam underwent charge exchange collisions, the cosine distribution assumed above would be seriously altered. Therefore calculations were made of the production rates of charge exchange ions from this source. These rates are negligible, even in the case of a Cs neutralizer used with a Cs thrust beam, which is the combination which has the highest charge exchange cross section.

c. Plasma Bridge Ions. Three questions arise with regard to the ion efflux from the discharge neutralizer: What is the ion energy, density,

and angular distribution? At this time only the first question can be answered with confidence. A properly operating discharge neutralizer has a plasma bridge potential of approximately 10 volts and the ions in this plasma have approximately 1/2 eV of kinetic energy.<sup>7,8</sup>

Since the energy threshold of sputtering yield is usually considered to be approximately 25 eV, these ions are only capable of causing erosion when attracted by negatively charged surfaces. (As a matter of fact, nearby accelerator plates, which are so charged, are often observed to erode preferentially in the neutralizer local. When the accelerator grid fields reach the plasma bridge, it is safe to assume that all escaping ions terminate on the grid.)

Probably the greatest threat from plasma bridge ions is that this plasma might extend to a solar array where charged conductors could draw significant ion or electron currents from it. This possibility should receive analysis.

9. Future Work. Progress during August will be limited by vacations and publication of the recently approved draft of last year's final report. Effort will concentrate on supporting thermophysics experiments and completion of the multipurpose sample holder.

#### B. Thermophysics.

1. Summary. During the 2nd quarterly period, work centered on the following tasks:

- (1) Finding a workable and practical solar simulation method.
- (2) Designing and fabricating a telescopic sight and simulator mounting structure for implementing the results of 1.
- (3) Designing, fabricating, and wiring the switching and control console.
- (4) Finishing fabrication details on the sample holder assembly.
- (5) Making pre-exposure ex situ spectral reflectance measurements.

- (6) Installing the sample holder assembly, reference radiometer, and solar simulator in and on the vacuum chamber.
- (7) Developing and debugging a data reduction computer program for in situ data.
- (8) Making preliminary checkout runs with the in situ test equipment.
- (9) Diagnosing and overcoming problems uncovered in (8).
- (10) Commencing degradation runs with five painted samples exposed to mercury neutrals.

These and other relatively minor activities are described individually in the following sections.

2. Solar Simulation. It was reported in the First Quarterly Report that a problem had been encountered concerning spectral non-uniformity of the Christie solar simulator beam. During May, several alternatives for dealing with this problem were investigated, and one was selected for use in the in situ test. The selected solution is to use only a 1.75 inch diameter zone near the center of the Christie beam and aim this zone onto each of the five samples and the radiometer one at a time. To do this, a telescopic sight has been mounted on the Christie and adjusted so that its cross hairs sight on the center of the usable zone at the sample plane. Sighting aids on each sample ion shield have been provided for this purpose. In addition, a new mounting structure has been designed and built for the Christie simulator. Figure 6 shows how this mount fastens directly onto the vacuum chamber bulkhead and provides fine angular adjustments in both the X and Y directions.

Spectral total flux density measurements were made at 1/2 inch intervals over a range of  $\pm 1.5$  inches in both the X and Y directions using the new telescopic sight on the Christie. Results from these measurements indicate that the spectral distribution is essentially uniform throughout the 3-inch diameter zone. A slight drop off of the  $0.88\mu$  peak relative to the intensity at other wavelengths was noted at the  $\pm 1.5$  inch positions in both the X and Y directions. Fortunately, this variation falls well beyond the edge of the 1.75 inch diameter samples.

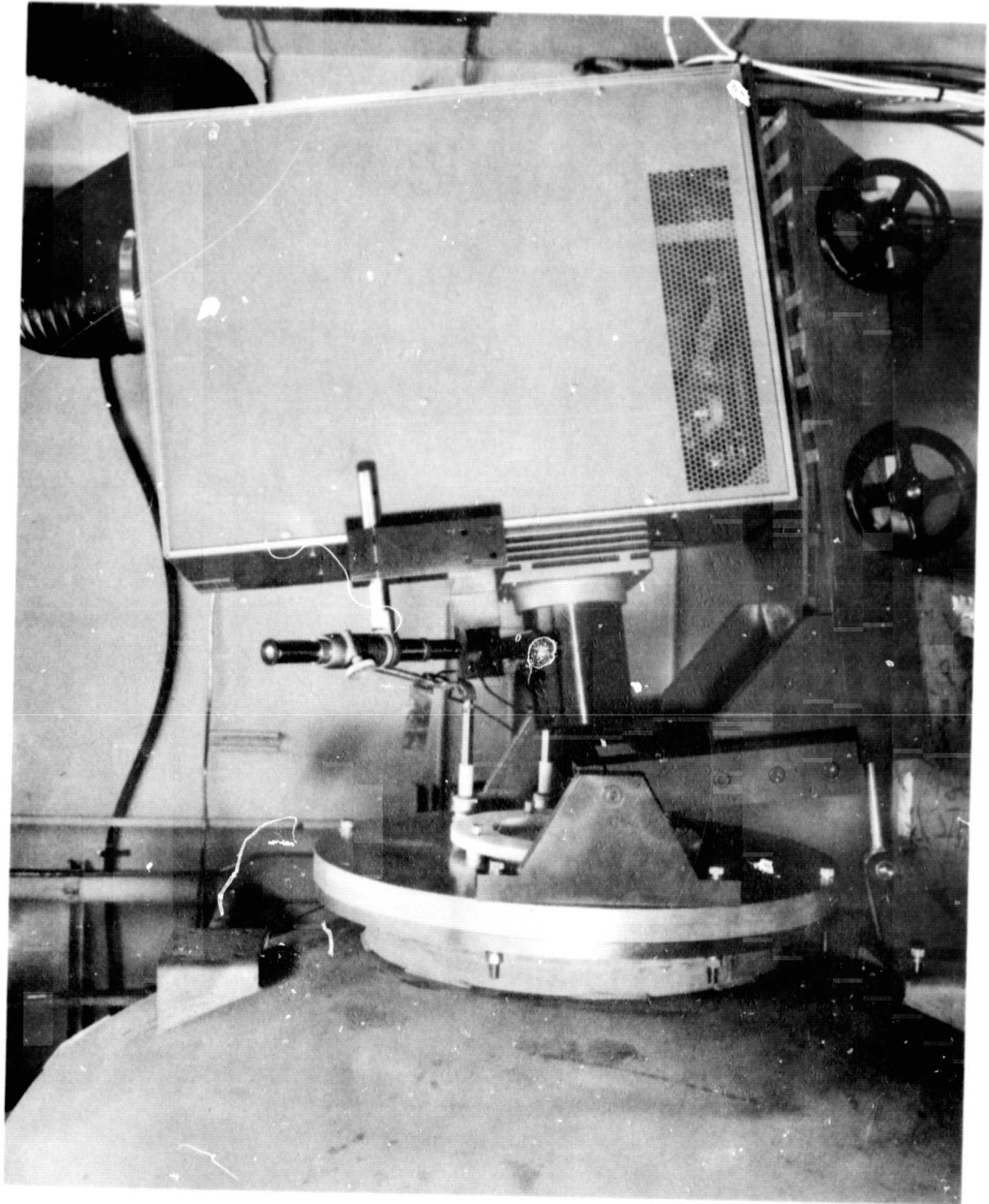


Figure 6. Solar Simulator on Adjustable Mount.

The distribution of total intensity (as measured by a radiometer with a 1.3 centimeter diameter aperture) is shown in Figure 7. It can be seen that the beam intensity is quite symmetrical about the center of the zone and that the intensity at a radius of 0.875 inches (corresponding to the edge of the 1.75 inch diameter sample), is approximately 11% lower than at the center. The ratio between the effective intensity and the center intensity will be considered as a constant correction factor. It has been determined by integrating the relative intensity distribution over the sample area and dividing the result by the sample area, as shown in Table I, with the result that  $I_{\text{effective}} = 0.94 I_{\text{center}}$ . Occasionally, total intensity of the beam will be remapped in situ and this correction recomputed.

3. Reference Radiometer. The TRW EC-1 has been selected for a reference radiometer. This is an electrically compensated radiometer which consists of two nearly identical foils housed in nearly identical enclosures. One foil is exposed to the unknown beam intensity through a 1.3 cm diameter quartz window. The other foil is heated electrically at a rate that will just null a differential thermocouple operating between the two foils. The beam intensity can be determined approximately from the measured electrical power, the window aperture area, the absorptivity of the receiving foil, and the transmission of the window. For greater accuracy however, several identical instruments have been calibrated in vacuum against a laboratory standard radiometer.

Figure 8 shows the radiometer as installed within the chamber. The radiometer aperture is in the same plane as the samples.

4. Switching Console Fabrication. The switching and control console for driving and monitoring the five sample holder units and the reference radiometer was completed during May. Switching circuits were added so that the automatic controller that nulls the sample package heat meters can also be used to balance the EC-1 reference radiometer. The total intensity measurements described in Section II.B.2 were made using the controller to drive the EC-1 radiometer. Figure 9 shows the entire electronics package including the switching console.

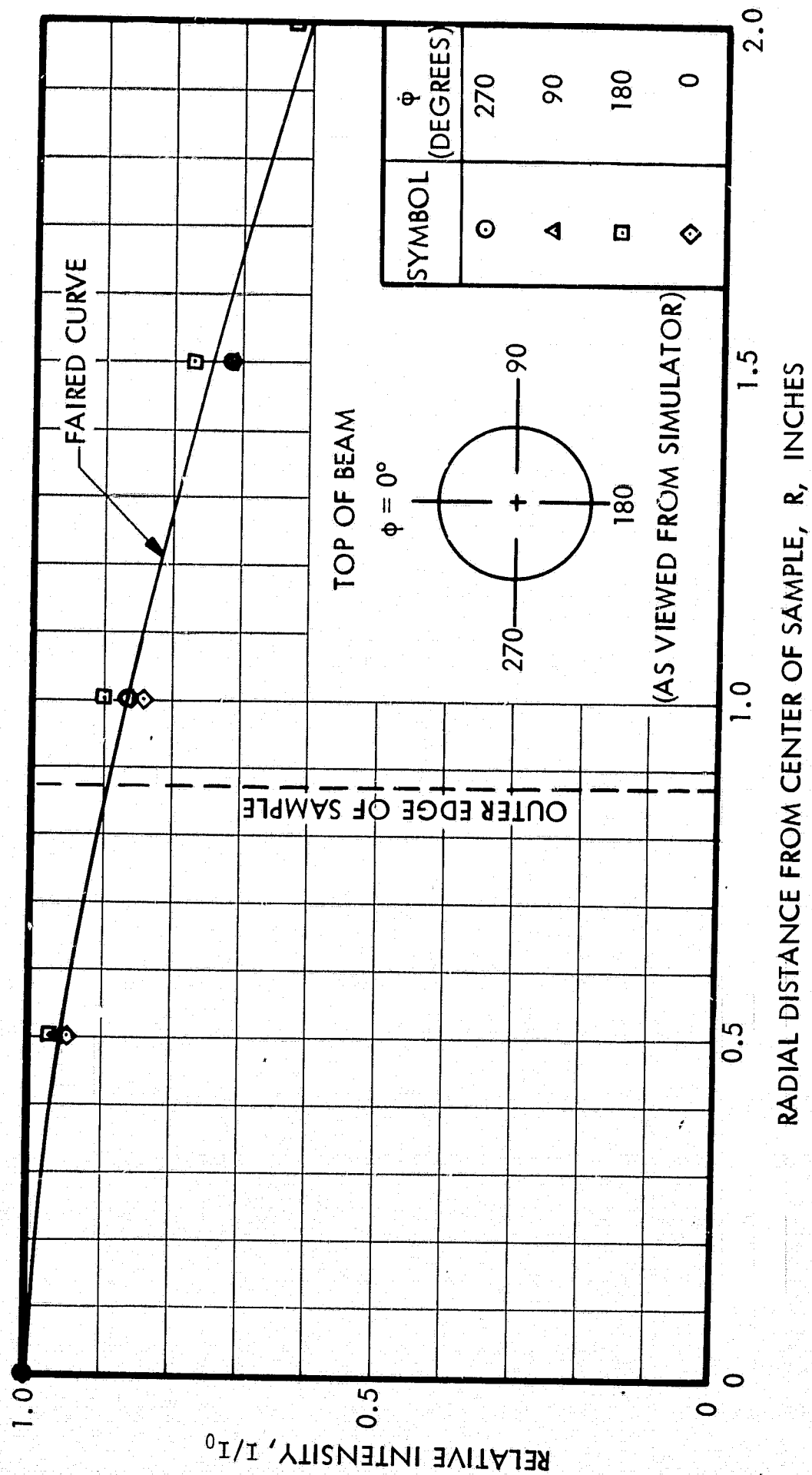


Figure 7. Total Intensity Distribution at 60.3 Inches From the Front Face of the Christie Lamp Housing.

TABLE 1  
COMPUTATION OF EFFECTIVE BEAM INTENSITY

$(\bar{R})$ (inches)	$(I/I_0)$	$\Delta R$ (inches)	$(\bar{R}) (I/I_0) (\Delta R)$
.05	.995	.10	.004975
.15	.990	.10	.01485
.25	.982	.10	.02455
.35	.975	.10	.034125
.45	.960	.10	.04320
.55	.949	.10	.052195
.65	.940	.10	.0611
.75	.912	.10	.0684
.8375	.899	.075	.05647
SUM		.875	.359865
$\frac{I_{\text{effective}}}{I_{\text{center}}} = \frac{2 \sum (\bar{R}) (I/I_0) (\Delta R)}{R_{\text{max}}^2} = \frac{(2) (.359865)}{(.875)^2} = 0.94$			



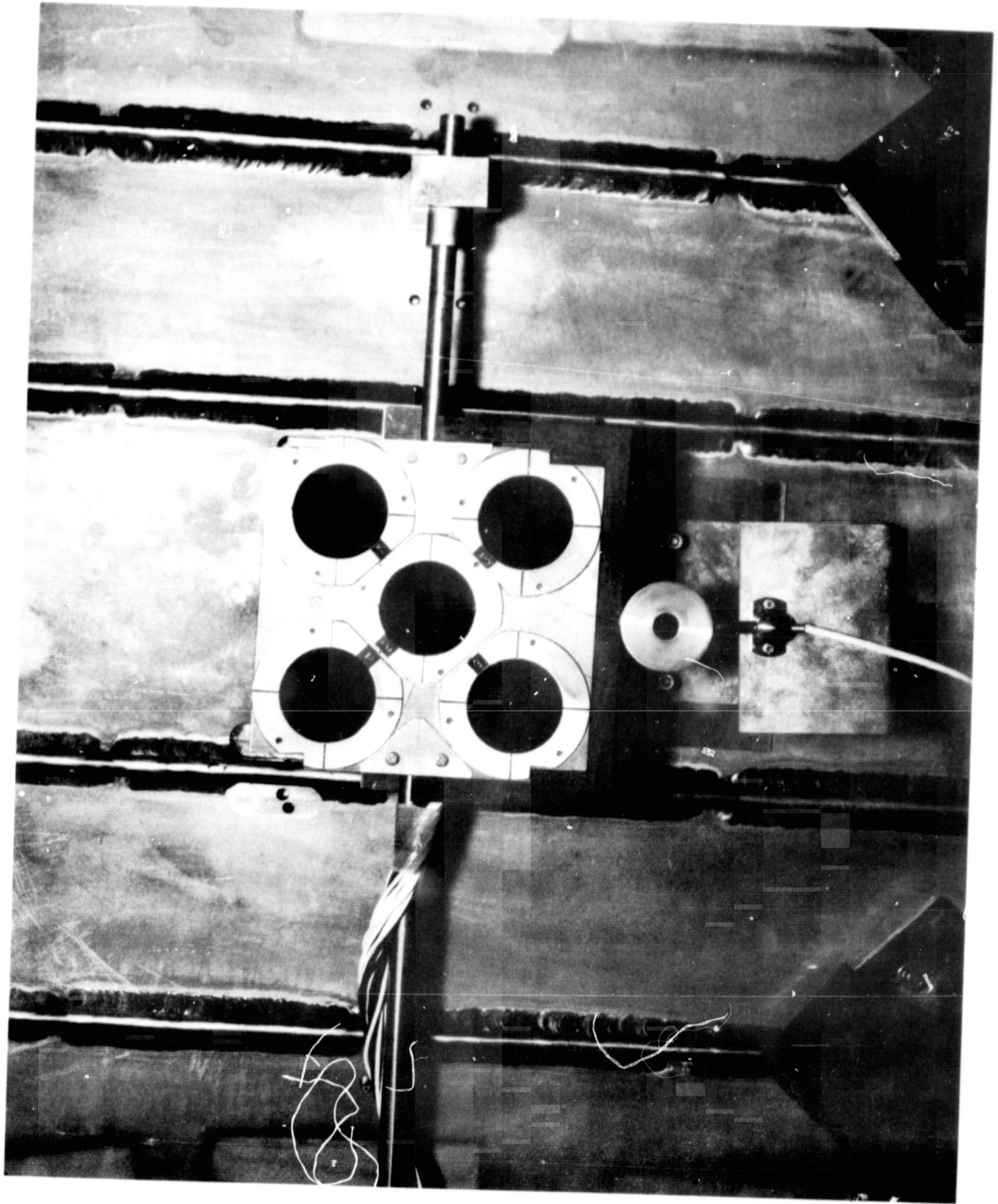


Figure 8. Surface Thermal Sample Holder in Measurement Position. Radiometer Appears Below Sample Holder.

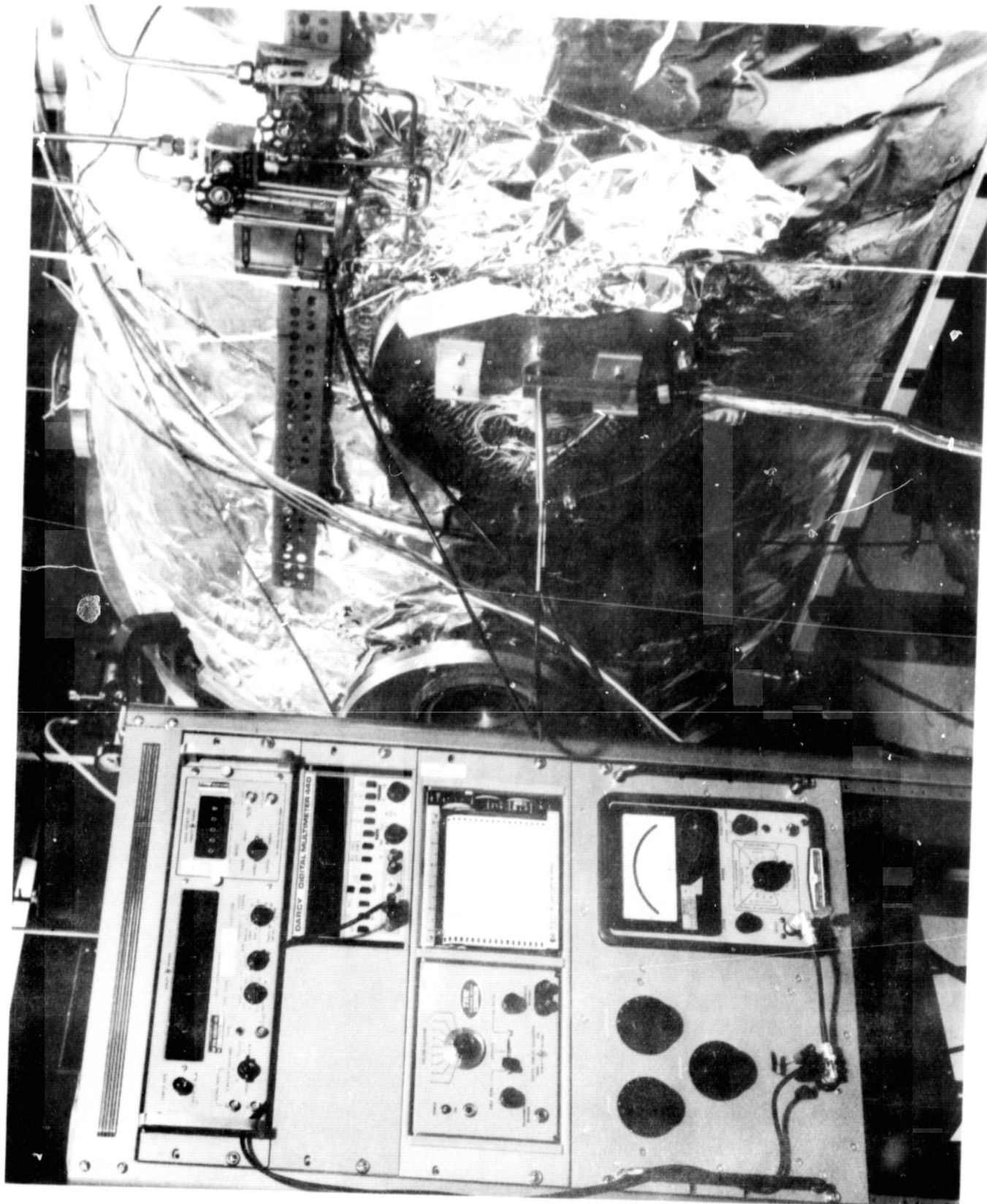


Figure 9. Exterior View of Port Plate, Electronics, and Water Cooling System.

Also visible in Figure 9 is the vacuum port cover plate which supports the sample holder package. This plate was machined and the mechanical and electrical hermetic seal pass-throughs were installed and wired during May.

5, Sample Holder Unit Fabrication. An ion shield has been fitted to each of the five heater-heat meter units. The shields are made of aluminum and are attached with RTV 165 to the copper heat sink plate. A gap of approximately .010 inch exists between each shield and the edge of the corresponding sample or heater. Small tabs of .010 inch thick mica have been bonded to the under side of each shield to protect electrical leads crossing the gap from being eroded. Figure 8 shows an external view of the ion shields. The four black lines on each shield are the sighting aids mentioned in Section II.B.2. The gap and the mica tabs are too small to be visible in the photograph. Two triangular pieces of aluminum are visible in Figure 8. These pieces cover reference mica tabs which can be easily removed, inspected for erosion and replaced. Each triangular piece has a .010 slit to simulate the gap between the sample and the ion shield. When these reference tabs wear thin the actual tabs will be renewed.

6. Sample Procurement and Preparation. As was indicated in the April quarterly report, most of the sample procurement and preparation has been completed. There were, however, three procurement events during this quarter that are worthy of reporting.

- (1) The Z93 and S13G samples were received from IIT and were found to be acceptable.
- (2) The Corning 7940 quartz and Corning 0211 microsheet discs which had been sent out for VDA (vacuum deposited aluminum) were received and found to be unacceptable due to incomplete coverage near the edge. They were returned for reprocessing and are now acceptable.
- (3) One hundred grams of RTV566 and 1.0 pound of RTV41 were ordered and received. Thirty aluminum discs are currently being coated with each type of RTV.

7. Ex Situ Measurements. Spectral reflectance of two specimens of each of the following sample materials has been measured.

Gold plating on 6061 T6 aluminum

Polished 6061 T6 aluminum

PV 100 white paint

Z93 white paint

Z13G white paint

Cat-a-Lac black paint

3M 401-C10 black paint

These measurements were made between 0.28 microns and 2.9 microns on the modified Beckman DK2A Spectrophotometer<sup>9</sup> and between 2.0 microns and 26 microns on the Gier Dunkle Heated Cavity.<sup>10</sup> In addition, two samples of each of the second surface mirrors (aluminized microsheet and aluminized quartz) have been measured between 0.28 microns and 2.9 microns on the modified Beckman DK2A. These samples cannot readily be run on the Heated Cavity.

8. In Situ Data Reduction Program. An in situ data reduction program was written and "debugged" during June so that data can be reduced immediately after being taken. This is necessary in order to determine whether or not the measurements should be repeated before proceeding with the experiment. It also allows immediate appraisal of what degradation if any was imposed on the thermal properties ( $\alpha_{xe}$  and  $\epsilon_H$ ) of the samples by the previous beam exposure. The program is operational and is currently being used even though all of the correction factors have not yet been determined and introduced into the program.

9. Preliminary Checkout Runs. In order to check out the operation of all of the equipment, checkout runs were made with samples whose properties are known. During the course of these runs several operational problems were encountered and overcome.

First, it was found that pressure and temperature fluctuations in the tap water caused 30-40 $\mu$ v fluctuations in the heat meter outputs. This problem was cured by converting to a gravity feed water supply system with a settling

tank and insulated lines. Heat meter fluctuations were thereby reduced to  $\pm 2\mu\text{v}$ .

The second major problem encountered was temporal instability of the Christie solar simulator beam intensity. The beam flux density was found to frequently go into an oscillatory mode with a period of about 2 minutes and a wave shape very similar to that of a full-wave-rectified sine wave. The cause of this oscillation is not known but the long period suggests that it may be due to thermal effects. Measurements of the power supply input voltage indicated no such oscillation. Two different power supplies were tried; one supplied essentially constant dc voltage and the other supplied essentially constant dc current but neither provided dc constant power, apparently because of temperature-induced fluctuations in the lamp characteristics. Christie engineers suggested that the lamp position relative to the spherical mirror may have been improperly adjusted so that the reflected arc image was focussing on the lamp electrodes. Since moving the lamp would jeopardize the spectral and total energy calibrations, this idea was checked out by inserting a piece of aluminum foil between the lamp and the spherical mirror. The two minute oscillation still persisted. The problem has been overcome by installing a high power transistor and resistor across the dc supply leads to provide a variable shunt. A silicon solar cell has been installed inside the lamp housing and its output controls the bias on the shunt transistor so as to maintain nearly constant output power, even when the lamp is oscillating.

The third problem has not been completely resolved. It involves an apparent zero off-set of about  $13\mu\text{v}$  on the differential thermocouple between the radiometer foils. A Hewlett Packard 425A electrometer is used to read the radiometer thermocouple as well as the heat meters. If the input to the electrometer is shorted and the instruments then set to read zero, one would expect to still read zero when the instrument is connected to the radiometer thermocouple with no flux applied to the radiometer. In fact, however, the electrometer reads about  $13\mu\text{v}$  under these conditions which indicates that either there is a thermal flux on the radiometer or spurious EMF is being generated somewhere in the system. The  $13\mu\text{v}$  off-set is only observed when the chamber liner is  $\text{LN}_2$  cooled, and is sensitive to external

heating or cooling of the feed through region of the port plate. This suggests that temperature gradients through the soldered pass through pins may be generating the EMF even though precautions were taken to avoid such EMF. If so, the temperature and heat meter readings may also be slightly in error due to the same effect. All of the preliminary check out runs were made with the electrometer set to read zero when the input was shorted. The effect of the zero shift would be felt most strongly on samples run at relatively low lamp intensity. Such samples include gold, polished aluminum and black paints.

10. Results of Preliminary Runs. Preliminary check out runs were made first with five 3M black velvet paint samples and then with five gold plated aluminum samples. Table II shows a comparison between the values obtained in situ and those obtained ex situ.

Table II. Summary of Results of Preliminary Check Out Runs.

Material	No. of <u>In Situ</u> Measurements	<u>In Situ</u>		<u>Ex Situ</u>		<u>In Situ</u>		<u>Ex Situ</u>
		$\epsilon_H$	Scatter	$\epsilon_N$	$\epsilon_H^*$	$\alpha_{xe}$	Scatter	$\alpha_{xe}$
3M Black Paint	5 (1 on ea. sample)	.88	$\pm .02$	.918	.870 $\pm .03$	.989	+ .005 - .015	.983 $\pm .015$
Gold Plated Aluminum	17	.046	+ .027 - .006	.023	.030 $\pm .02$	.218	+ .081 - .028	.130 $\pm .015$

\* $\epsilon_H$  calculated from normal emittance inspection measurements using the theoretical correlation given in Eckert and Drake "Heat and Mass Transport" 2nd Ed.

In situ results shown in the above table do not include any correction for edge-loss nor do they include correction for thermocouple calibration deviation from the standard NBS table. The intensity non-uniformity factor (0.94) discussed in Section II.B.2 was included for all runs in which the simulator lens was in place. A few runs were made with the gold samples during which the lens was removed. In these cases the intensity was uniform across



sample so the 0.94 factor was not applicable. The final results with and without the lens were in good agreement.

11. Exposure of Paints to Atomic Mercury Beam. Thermal properties of five samples (Cat-a-Lac black paint, 3M black paint, 3M black paint, PV100 white paint, Z93 white paint, and S13G white paint) have been measured in situ before and after exposure to mercury neutrals. Preliminary results are that  $\alpha_{\text{xenon}}$  and  $\epsilon_H$  were unchanged on the white paints after a total exposure of 4.425 hours of  $10^{14}$  atoms  $\text{cm}^{-2} \text{sec}^{-1}$ . The  $\epsilon_H$  value for the black paints also showed little or no change, but  $\alpha_{\text{xenon}}$  for both black paints appears to have been reduced by about 3 to 10% after only 1.75 hours of exposure. Further exposure to 4.425 hours caused little or no change.

These findings are strictly tentative because early results from the degradation runs indicate considerably more data scatter on the in situ  $\alpha_{\text{xenon}}$  of black paints than was experienced during the preliminary check out runs. White paints which are run with almost ten times as much beam intensity as the blacks show very little  $\alpha_{\text{xenon}}$  data scatter. This suggests that the scatter problem may be in the beam flux density measurement -- possibly related to the electrometer zero off set problem that was discussed in Section II.B.9. Another possibility is that mercury may have gotten into the radiometer connector. These and other possibilities are being investigated.

12. Work Planned for Next Period.

- 1) Finish preparing the RTV 566 and RTV 41 samples.
- 2) Run ex situ measurements on the RTV samples.
- 3) Continue degradation runs first with mercury neutrals then ions. These tests are being postponed 2 weeks because of vacations.



## C. Chemistry

1. Summary. Sylgard 182, Delrin, GT100, SMRD 745, Teflon FEP and Kapton H-film were selected for cesium and mercury immersion tests as these materials are representative of the chemical structures making up the organic matrices of the spacecraft materials under study. All samples were immersed in cesium and in mercury for 48 hours at room temperature and the chemical effect of the metal was analyzed by thin-layer chromatography, appearance, weight gain or loss and infrared spectroscopy. It was found that mercury had no apparent interaction with any of the spacecraft materials. In the case of immersion in cesium, it was found that Teflon FEP was totally degraded, at the surface, to carbon, Kapton H-film formed a one electron oxidation-reduction salt with cesium, while Sylgard 182, Delrin, GT 100 and SMRD 745 were unaffected by cesium. Three adhesives were tested for ability to cement thermoset spacecraft material film to an aluminum surface (a necessary prerequisite for exposure of films in the multipurpose sample holder). Acetate adhesive was selected as it cemented H-film to aluminum surfaces and retained its binding power for 24 hours at 25 microns of pressure, and the Kapton H-film could be easily peeled from the substrate, without damage, for analysis.

### 2. Discussion and Results

a. Cesium Immersion. Six materials were selected as representative of most of the organic materials used in spacecraft construction. These are Kapton H-film, Sylgard 182, GT 100, Delrin, SMRD 745, and Teflon FEP. Each of these materials was dried in a sample tube at 90-100°C/25  $\mu$  for one hour just prior to distillation of the Cs onto it. Each material was left in the liquid metal at approximately 30°C for 48 hours. In addition, the H-film was exposed to Cs at 30°C for 48 hours while in tension and also at 60°C for 48 hours.

At the end of the exposure period each material was washed with reagent n-hexane and then quenched in reagent methanol. The samples were dried and weighed to determine weight loss or gain. Control samples were given identical treatment except for cesium exposure. Infrared spectrograms were made of all samples using the ATR device.

The exposure of SMRD 745, Delrin, Sylgard 182, and GT-100 produced little if any change in the appearance of the materials. In all cases exposure of the H-film produced a deep violet color where the Cs touched the surface of the material. No differences were noted between these test results and the 22°C, 48 hour exposure previously reported. The physical properties of the exposed film had not changed after quenching. As long as the samples were protected from moisture the color remained, but when they were exposed to laboratory air, the color disappeared over a period of days. The exposure of Teflon FEP produced a major and lasting change in the surface properties of this material. The surface of this material had turned black and the sample lost approximately 2% of its weight. The infrared spectrum of the exposed sample indicated the destruction of the C-F bonds at the surface.

The thin film chromatographic analysis of the condensed wash and quench solutions did not show the presence of organic materials in them. Acidification of these solutions did not change this. This indicates that in none of the cases, did organic residues break off the polymer chains nor was there any extensive lowering of molecular weight. Quantitative results are listed in Table III.

Table III. Preliminary Analysis of Cesium Exposed Spacecraft Materials

Material	Initial wt., g	Final wt., g	Percent wt. Changes	Comments
Delrin <sup>1</sup>	1.2145	1.2153	+0.066	no visible change
Delrin <sup>2</sup>	1.3263	1.3272	+0.068	
Sylgard 182 <sup>1</sup>	0.1262	0.1255	-0.55	no visible change
Sylgard 182 <sup>2</sup>	0.1164	0.1154	-0.86	
Teflon FEP <sup>1</sup>	0.2601	0.2543	-2.23	sample turned black
Teflon FEP <sup>2</sup>	0.2481	0.2480	-0.04	
SMRD 745 <sup>1</sup>	0.5982	0.5844	-2.31	no visible change
SMRD 745 <sup>2</sup>	0.6056	0.5930	-2.08	
GT 100 <sup>1</sup>	0.0624	0.0587	-5.02	no visible change
GT 100 <sup>2</sup>	0.0638	0.0624	-2.19	

1. Exposed (immersed in cesium, then immersed in quench solution and dried).
2. Standard unexposed (immersed in quench solution and dried).

Except for the H-film and Teflon FEP there is no evidence that the materials tested undergo rapid degradation.

It has been postulated that the H-film undergoes a one electron oxidation-reduction which produces the observed purple color on the surface of the film. It is also expected that the salt produced would be electrically conductive.

The reaction of Cs with the Teflon FEP film apparently proceeds with the extraction of fluorine from the surface of the polymer. This leaves a carbon surface which will conduct electricity and also provides a breakdown path for high voltages after short reaction times. The blackening of the surface should radically affect the emission-absorption properties of the material.

b. Mercury Immersion. Weighed samples of each of the six selected materials were placed in clean reaction tubes and covered with freshly filtered triple distilled mercury. At the end of 48 hours, the mercury was decanted from the tubes and the samples were flushed with reagent hexane. After drying, each sample was visually inspected and reweighed.

Sample	Weight g		% Change
	Before Exp.	After Exp.	
H-film	0.0572	0.0584	+0.35
GT-100	0.0573	0.0582	+1.22
Sylgard-102	0.1111	0.1114	+0.27
Delrin	1.2156	1.2157	+0.008
Teflon FEP	0.1105	0.1108	+0.27
SMRD 745	0.5597	0.5606	+0.16

Visually there were no indications of reaction between the materials and the metal. Small increases in the weight of each sample were noted. This is probably due to the adherence of small amounts of mercury to the surface of the samples. The surface of the GT-100 is rougher than those of the others and it also has a larger surface to weight ratio. This explains the larger weight change for this sample.

These experiments indicate that there is little or no reaction between the selected materials and metallic mercury at room temperature for the time interval of the tests.

c. Adhesive Experiments. A short investigation was undertaken to determine a good adhesive to fix samples to the holders for the ion exposures.

The criteria was that a good bond be formed, but the sample be capable of being freed without damage.

Experiments were carried out with H-film. Films (3/4" x 1") of this material were glued to aluminum sheet and tested for adherence manually. The samples were subjected to shear and peeling tests.

Three materials were tested, vinyl alcohol (dissolved in water), ethyl cellulose (dissolved in ethyl alcohol), and vinyl acetate emulsion to which ethyl alcohol was added.

The aluminum plate was coated with the desired adhesive and the film was pressed firmly down on it. The sample was then dried at 40-50°C approximately 1/2 hour, and then given a manual shear test, which consisted of taking the sample in the right hand and producing a shear stress on the adhered film with the right thumb.

It was found that the vinyl acetate emulsion gave the best bond. The vinyl alcohol material did not dry even after several hours and the ethyl cellulose gave a poor bond.

A final test was conducted on the vinyl acetate material. A well handled sample was placed in a vacuum chamber and held for 24 hours at approximately 25  $\mu$  pressure. At the end of this period, the sample was still well bonded to the aluminum sheet, but could be peeled from the substrate without damage.

3. Future Work. Future work in the chemistry work unit will consist of ex situ chemical analysis of selected samples which have been exposed to propellant beams within the 4 x 8 foot vacuum facility as they become available.

#### D. Metallurgy

1. Immersion Tests. During the Quarterly reporting period immersion tests have been completed on the metallic combinations silver/mercury, solder/mercury, and solder/cesium as summarized in Table IV. These exposures were made in the test vessels described in earlier reports. The mercury tests were performed in air, whereas the cesium tests were performed under vacuum.

a. Solder in Mercury. The eutectic solder/mercury tests were terminated after 6 weeks of exposure. The sample volume was approximately one-half its initial value. As mentioned in the First Quarterly Letter, the glass walls of the test vessel were coated with a metallic precipitate. Formation of a precipitate is the necessary result of dissolving a large quantity of solder constituents, since mercury can only hold 1 to 2% of either lead or tin in solution at room temperature.

Metallographic examination of this sample was not possible because the solder had taken a substantial amount of mercury into solution and did not have sufficient mechanical strength to be mounted and polished. Visual examination of the sample verified that it contained a large amount of mercury. This result is consistent with the phase diagrams for the combinations Pb/Hg and Hg/Sn. These phase diagrams show that Pb will take up to 24% Hg in solution and Sn will take up to 10% Hg at room temperature. The phase diagrams do not indicate rates of reaction; they indicate what will result after reactions are complete. The immersion tests demonstrated that a six week exposure of solder to excess mercury produces a structure with little or no mechanical strength.

Table IV. Immersion Tests Complete  
During Reporting Period

<u>Combination</u>	<u>Duration of Test</u>
Solder/Mercury	6 weeks
Silver/Mercury	4 weeks
Solder/Cesium	< 72 hours
Solder/Cesium #2	5 days

b. Solder in Cesium. The eutectic solder/cesium immersion test sample was a 6 gram cylindrical casting. The sample was sealed in a test vessel, and the vessel was loaded with approximately 7 grams of cesium using the distillation system described previously. This quantity of cesium completely immersed the sample. Within the first hour after filling, a dark precipitate was seen to form on the internal glass surfaces. Visibility of the sample was lost due to cesium wetting the glass in the sample area. An attempt was made to remove this cesium by heating the vessel with a hot air gun. This attempt was only partially successful; however, the sample appeared to have only a surface coating of cesium. No reaction was visible at this time. Sometime within the next 72 hours a catastrophic reaction took place, breaking the glass vessel. It is not clear if the reaction was solely that of solder with cesium, or a partial reaction which caused the glass to crack, thereby exposing the cesium to air and causing a cesium fire which melted the solder. There was some evidence that a cesium fire had occurred and only a small amount of the solder sample remained. It was a melted button. The balance of the solder had reacted to form what appeared to be a cesium-metal hydroxide. A repeat test of the solder/cesium was performed to verify the catastrophic reaction of this combination. The sample was sealed in a modified test vessel. The modification used was to shorten the support platform to leave a reaction chamber that was approximately 3 inches long. The vessel was then loaded with approximately 8 grams of cesium using the distillation system. The cesium completely covered the solder sample and filled approximately 1/3 of the reaction chamber. Since the sample was covered with cesium no reaction could be seen, however, the cesium appeared to change in color from a metallic silver to a straw yellow. This color change was accompanied by a volume increase. No heat was applied to the test vessel and the dark precipitate was not seen. After 72 hours of exposure no apparent change could be seen in the sample. At this time the test vessel was heated to approximately 100°F. The yellow compound melted exposing what appeared to be the reacted solder slug. Upon removal of the heat the cesium compound resolidified with the same straw yellow color. After 5 days the test vessel was opened to air, which resulted in a cesium fire. However, the solder sample was

removed before melting could occur. Examination of the solder revealed that it had been severely attacked by the cesium but not in the manner as the previous sample. A photograph of the sample is shown in Figure 9. The remaining sample was then prepared for metallographic analysis. Photographs of the cross section is shown in Figure 10. The sample was prepared using standard metallographic techniques and was etched with a  $\text{HNO}_3 - \text{CH}_3\text{COOH}$  mixture. The edges appear to have been attacked at a relatively uniform rate and no apparent intergranular corrosion is noted. The cause of the catastrophic reaction that was observed in the first solder/cesium sample is apparently due to expansion of the solder/cesium compound against the test vessel and its support column which caused the glass to crack exposing the cesium to air. However, in both experiments the cesium attacked the solder at a rate which would probably preclude the use of solder at locations on the spacecraft which receive high arrival rates of cesium.

c. Silver in Mercury. The silver-mercury immersion test was terminated after 4 weeks. Upon removal of the silver sample from the mercury, a surface coating of mercury was still present. The sample was cleaned by rubbing it in sulfur, which formed a Hg-S compound, washing this compound off with water, and then briefly immersing it in dilute nitric acid. The sample was then measured and weighed. There was no apparent change in physical dimensions of the sample but there was a slight weight gain due either to incomplete removal of the surface coating of mercury or to mercury being dissolved into the silver. According to the Ag/Hg phase diagram, silver can take approximately 30% mercury into solution.

Cross sections of the silver sample before and after mercury exposure are shown in Figure 11. Surface irregularities such as that appearing in Figure 11b were also seen in the unexposed sample. Therefore, they are not ascribed to mercury exposure. Most of the outer edge of the exposed sample has approximately 0.2 mil layer of porous-appearing material. Occasionally there are local regions where this layer is approximately 2 mils thick, such as the one shown in Figure 11b. The zone underneath the surface layer,

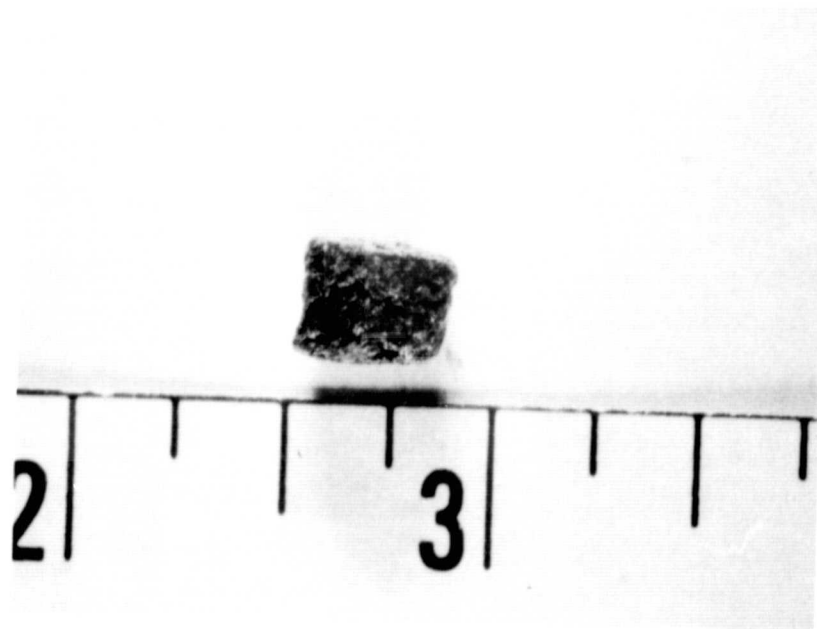


Figure 9. Solder Sample After 5 Day Exposure to Cesium.

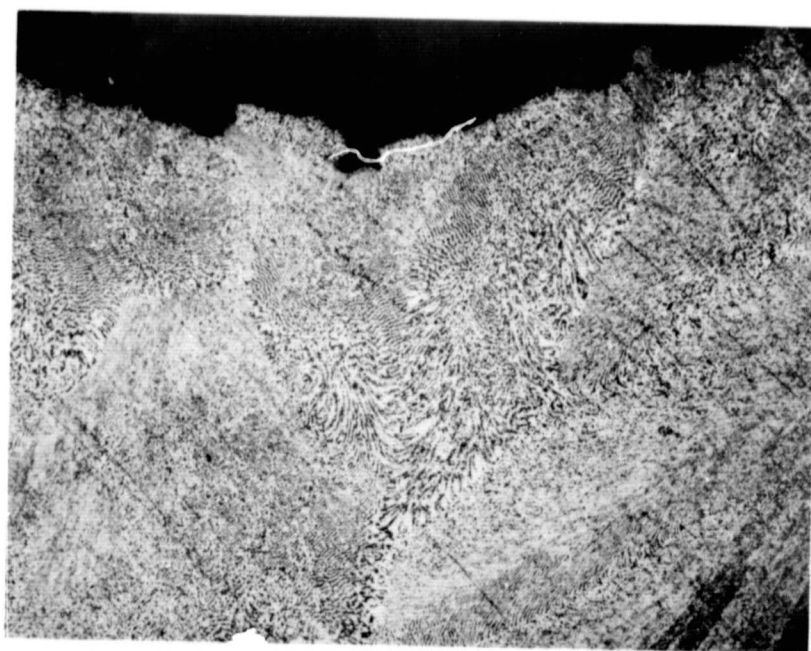


Figure 10. Cross Section of Solder Sample After Exposure to Cesium. 100X.



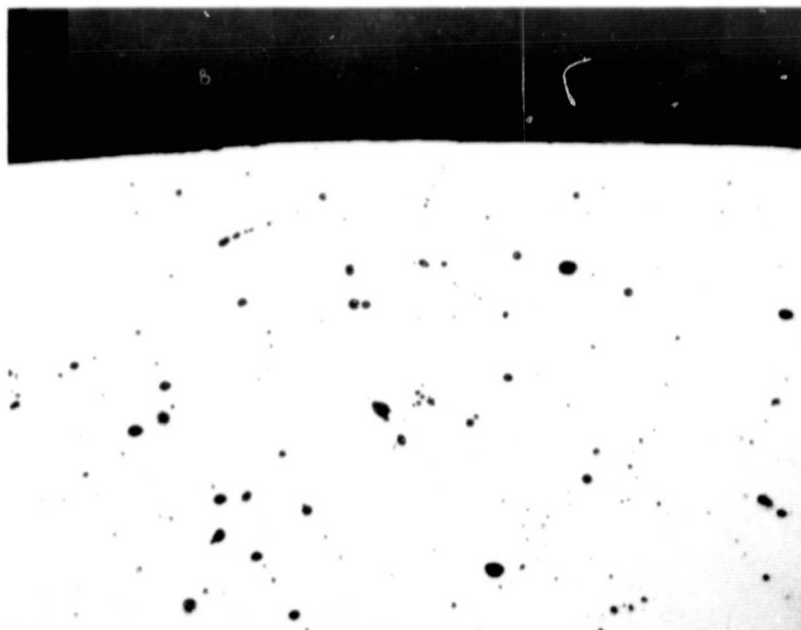


Figure 11a. Cross Section of Silver Casting  
Before Exposure to Mercury. 100X.

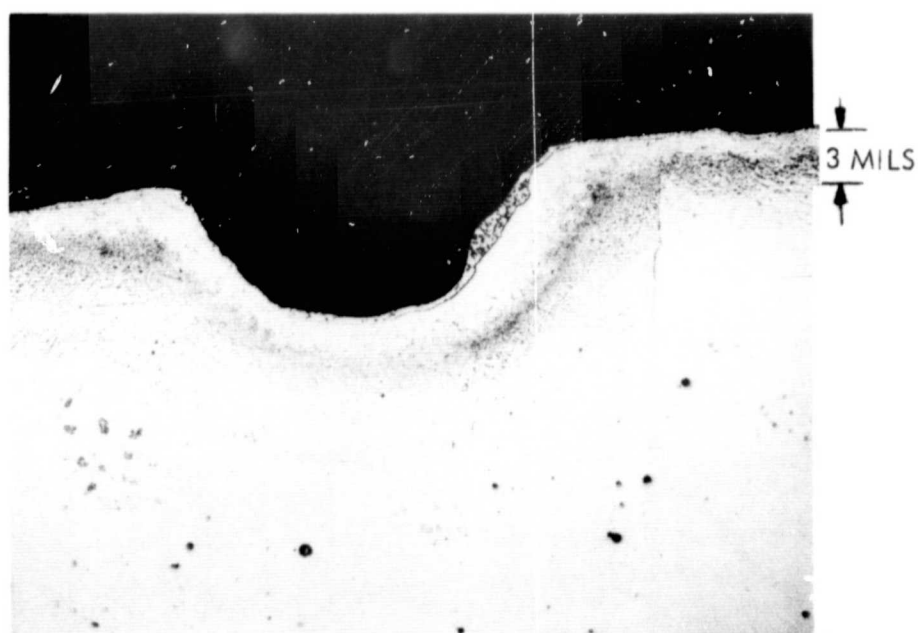


Figure 11b. Cross Section of Silver Casting  
After 4 Week Exposure to Mercury. 100X.

which is defined by the dark band, has an average depth of approximately 3 mils. Interpreting these preparations in terms of the phase diagram, one expects that the outer layer is  $\epsilon$  phase (containing approximately 45 A% Hg), and that the zone underneath is a solid solution ranging in mercury concentration from 36 A% at the interface with the  $\epsilon$  down to approximately 0% somewhere in the vicinity of the dark band. A series of microhardness measurements were performed on the silver sample after exposure to the mercury. Table V lists the relative hardness of the sample from the center toward the edge. As predicted, the hardness does increase as the traverse is taken with the hardest point at the edge of the sample. Figure 12 is a photograph of the microhardness indentations.

2. Mechanical Properties Testing. The mechanical properties test of

a. Solder. The mechanical properties test of solder was performed on samples which were machined into 1/4-in. thick tensile bars. One bar was tested as machined; two identical bars were exposed to mercury and then allowed to diffuse at room temperature for periods of one week and one month. Tensile tests were performed after these time periods. The exposure of the samples was performed by forcing solvent cleaned test bars of solder into the mercury and allowing the buoyant force to expell the samples from the mercury. The total time in the bulk of the mercury was that required to push the solder to the bottom of the mercury container and be pushed out by the buoyant force. The solder bars wet completely with a thin surface coating of mercury and appeared as a front surface mirror. The coated samples were then stored at room temperature. Before testing visual observation indicated that the thin surface coating of mercury had diffused into the bulk of the sample. The surface at this time was a dull solder gray. The samples were then tensile tested in a standard method using a crosshead speed of .05 in/min. Table VI presents the results of the tensile tests. The small variations in results between the one week sample and the unexposed sample may be largely statistical scatter. However, the third sample shows a marked decrease in elongation, decrease in tensile strength, and an order of magnitude change in modulus. These changes in mechanical properties indicate a change in the structure of the material with only a small coating of propellant.

Table V. Microhardness of Silver Sample After  
4 Week Immersion in Mercury

Location	Knoop Hardness
Center of sample	49.23
Middle of silver area	48.3
Interface	49.23
Diffusion zone	48.65
	59.23
	63.24

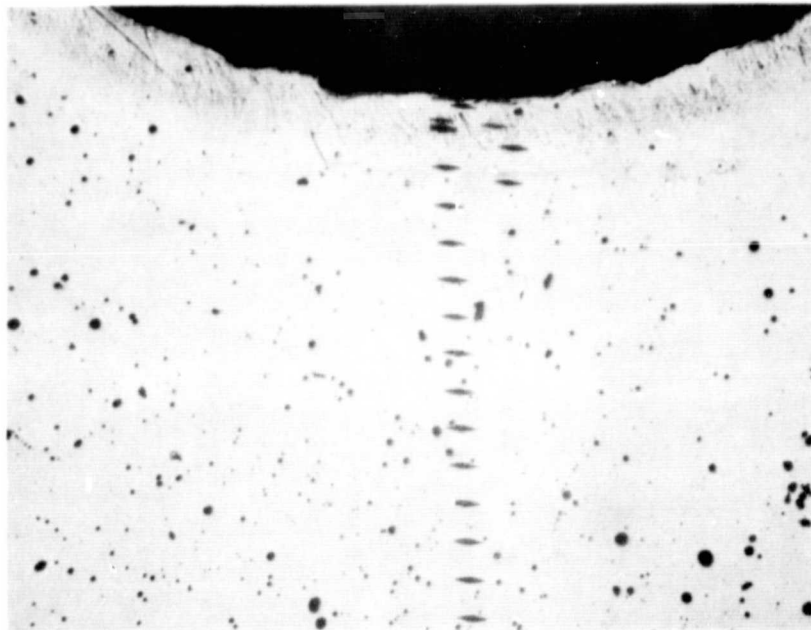


Figure 12. Microhardness indentation performed  
on Ag/Hg sample 100X.

TABLE I

Tensile Properties of Solder Test Bars

UNCOATED BAR

Yield Strength	2,200 psi
Ultimate Tensile Strength	4,200 psi
Elongation	90%
Modulus	$36.4 \times 10^4$ psi

COATED BAR - After 1 week exposure

Yield Strength	2,600 psi
Ultimate Tensile Strength	4,600 psi
Elongation	90%
Modulus	$32.5 \times 10^4$ psi

COATED BAR - After 4 week exposure

Yield Strength	2,450 psi
Ultimate Tensile Strength	3,300 psi
Elongation	29%
Modulus	$28 \times 10^5$

A further study of the mechanical behavior of solder in mercury was performed on a thin sheet (.007") tensile bars of eutectic solder. The bars were 1/4 inch wide in the center section and 4 inches in overall length. This solder was surface treated in the same manner as the large samples so that only a small amount of mercury would come in contact with the solder strip. The appearance of the strip after coating was identical to the large samples. In trying to move the samples after coating it was found that the samples would not support their own weight. The total time between coating and failure being less than 20 seconds. Figure 13 and 14 show solder samples after coating and then after fracture. Repeated tests showed that the longest period of time for the 7 mil sheet to fracture was less than one minute.

In considering the results of the three types of tests with solder and mercury -- long term immersion, surface coating of massive bars, and surface coating of thin bars -- the following picture emerges. When small quantities of mercury are present in solder, the solder is embrittled, as was shown by the fragility of the thin bars and the measured properties of the four-week thick bar. However when the mercury concentration becomes large, solder has little mechanical integrity: The sample which underwent 6 weeks of immersion was so "mushy" it couldn't be mounted and polished for metallographic examination.

Solder used on light weight solar arrays must be able to sustain both residual strain present at a joint after fabrication and strain introduced by handling, deployment and flexing. These experiments show 1) mercury "wets" solder so no advantage may be expected from low fractional monolayer adsorption energy and 2) limits will have to be imposed on the total amount of mercury arriving at exposed eutectic solder surfaces on solar-electric spacecraft.

b. Silver. After observing the changes in properties of the solder, a change from bend tests to tensile tests in the silver investigation was made. This decision was based upon the ability to obtain quantitative data from a tensile test, rather than the qualitative data that a bend test would provide. Silver tensile bars are being machined for testing in the next reporting period.

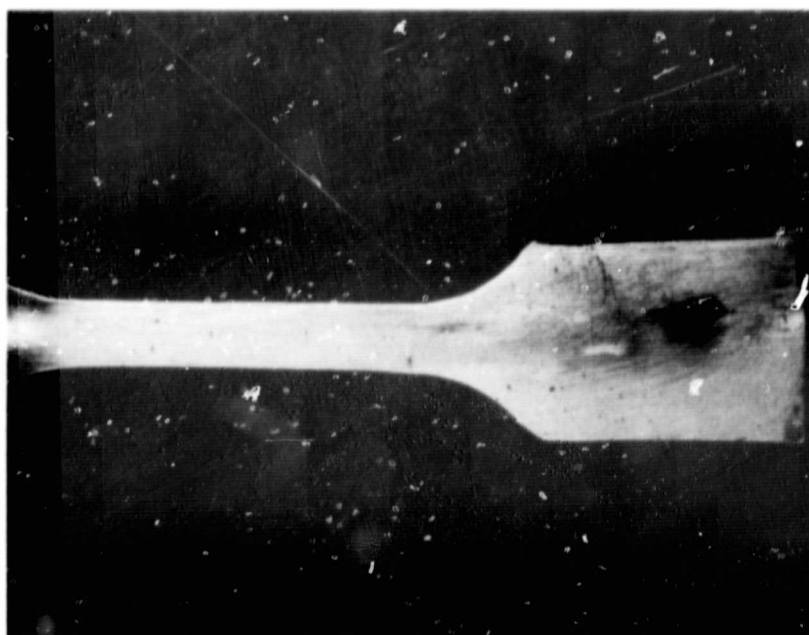


Figure 13. 7 mil Solder Sample After Surface Coating of Mercury.

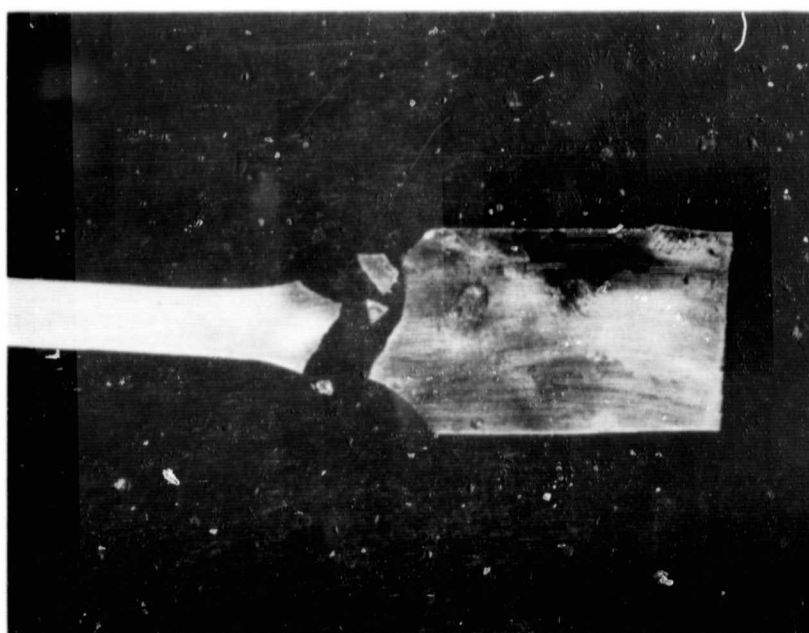


Figure 14. Fractured 7 mil Solder Samples.

3. Future Work. During the forthcoming reporting period the silver tensile bars will be exposed and tested. In accordance with the direction of the Technical Manager, solder alloys containing up to 10% silver will be prepared for testing in both mercury and cesium.

### III. CONCLUSIONS

The program is progressing satisfactorily through the final fabrication and initial experimental phases in each of the four work unit areas.

Techniques have been developed to circumvent the unexpected spectral nonuniformity and temporal instability of the xenon solar simulator.

Planned immersion testing of six representative organic spacecraft materials in liquid cesium and mercury have been completed. These materials are Sylgard 182, Delrin, GT100, SMRD 745, Teflon FEP, and Kapton (H-film).

Immersion of Teflon FEP in cesium for 24 hours at approximately 20°C produced a black, carbon surface layer through destruction of C-F bonds at the surface. This layer will conduct electricity and it provides a breakdown path for high voltages. If it is produced when Teflon is exposed to atomic cesium beams, then Teflon's use as an electrical insulator on spacecraft surfaces must be correspondingly restricted.

Results of immersing Kapton under tension in cesium for 48 hours at 30°C and relaxed for 48 hours at 60°C were similar to those reported in the First Quarterly letter. Therefore the conclusions stated there remain in force. As with Teflon, exposure of Kapton to atomic cesium beams is expected to establish measurable degradation rates.

The remaining four materials immersed in cesium and all materials immersed in mercury were not measurably affected. Consequently, it is expected that chemical effects of atomic beams impinging on these (and similar) materials will be either subtle or nonexistent.

Immersion of eutectic solder in both cesium and mercury resulted in heavy attack and in the case of mercury marked decrease in ductility as well as a decrease in strength. Even the application of a thin surface coating of mercury on solder tensile bars weakened them. Therefore restrictions on the use of solder on spacecraft surfaces are expected to result from atomic beam experiments.

A metallurgical reaction between silver and mercury has been observed. However the reaction rate is not rapid nor the properties of the reaction products obviously unacceptable.

Analysis of discharge neutralizers indicates that in a cone about its axis particle fluxes may be comparable to those from the thruster at high angles. The most potentially deleterious effect of plasma bridge ions is believed to be electrical, but this possibility deserves further analysis. These matters deserve consideration when choosing the orientation of a discharge neutralizer during spacecraft design.

#### IV. RECOMMENDATIONS

It is recommended that the potential deleterious effects of ions originating from discharge neutralizers receive additional analysis.

#### V. NEW TECHNOLOGY

None

#### VI. REFERENCES

1. First Quarterly Letter, #08965-6004-R000, Contract NAS7-575.
2. Second Quarterly Letter, #08965-6007-R000, Contract NAS7-575.
3. Third Quarterly Letter, #08965-6010-R000, Contract NAS7-575.
4. Final Report NAS7-575.
5. D. F. Hall, B. E. Newnam and J. R. Womack, "Electrostatic Rocket Exhaust Effects on Solar-Electric Spacecraft Subsystems," AIAA Paper No. 69-271, Mar. 1969.



6. L. B. Loeb, THE KINETIC THEORY OF GASES, p. 308, McGraw Hill, 1934.
7. G. A. Csiky, "Investigation of a Hollow Cathode Discharge Plasma," AIAA Paper No. 69-258, Mar. 1969.
8. D. F. Hall, R. F. Kemp and H. Shelton, "Mercury Discharge Devices and Technology," AIAA Paper No. 67-669, Sept. 1967.
9. W. D. Miller and E. E. Luedke, "In Situ Solar Absorptance Measurement, An Absolute Method," Effects of the Space Environment on Materials, Vol. 11, pp. 75-84, Society of Aerospace Material and Process Engineers, 11th National Symposium and Exhibit, St. Lou April 1967.
10. R. V. Dunkla, et al., "Heated Cavity Reflectometer for Angular Reflectance Measurements," Progress in International Research on Thermodynamics and Transport Properties, American Society of Mechanical Engineers, pp. 541-67 (1962).